Applicability of Recent Low-Cost GNSS Receivers to Deformation Monitoring

Katarzyna STĘPNIAK, Jacek PAZIEWSKI, Rafał SIERADZKI, Radosław BARYŁA, Poland

Key words: GNSS, low-cost receiver, positioning, deformation monitoring

SUMMARY

The continuous development of low-cost Global Navigation Satellite Systems (GNSS) chipsets and advances in processing algorithms that address the limitations of such hardware enable the exploitation of mass-market receivers in new fields of engineering and science. The ubiquitous presence of such devices is a factor that can particularly stimulate innovations and thus open the door to new applications for low-cost GNSS receivers. In this study, we focus on the actual positioning performance of recent mass-market GNSS receivers. In particular, this study aims to verify whether the low-cost receivers may be employed for precise deformation monitoring and reach an accuracy level close to that of high-grade receivers.

The experiment is based on GNSS observations collected using the most recent multi-frequency GNSS low-cost receivers provided by u-blox, Skytraq, and Septentrio. They are connected to two different types of GNSS antennas, a patch one dedicated to the low-cost receivers and the TRM59800.00 choke ring one. In addition, Trimble Alloy, which is a high-grade geodetic receiver, is also employed and treated as a benchmark in this study. GNSS data collected during the experiment are processed in Bernese GNSS Software v.5.2 in a relative mode. Developing an optimal processing strategy suitable for deformation monitoring with low-cost GNSS receivers was necessary to achieve the highest possible accuracy. This was done by extensive testing and selection of the most appropriate type of observations and their linear combinations, elevation cut-off angle, ambiguity resolution strategy, network geometry, troposphere, and ionospheric delays handling, etc.

The results show that with the optimal low-cost receiver data processing strategy, the latest low-cost receivers may be considered a mature complement to high-grade receivers in engineering applications, such as deformation monitoring.

Applicability of Recent Low-Cost GNSS Receivers to Deformation Monitoring

Katarzyna STĘPNIAK, Jacek PAZIEWSKI, Rafał SIERADZKI, Radosław BARYŁA, Poland

1. INTRODUCTION AND MOTIVATION

The Global Navigation Satellite System (GNSS) has been widely used in the last decades for geodetic monitoring where high accuracy and precision are needed. Therefore, geodetic class equipment is usually employed in these applications allowing to achieve accuracy in the order of millimetres (Larson et al., 2010; Baryla et al., 2014; Wang et al., 2014; Martín et al., 2015). However, the high quality and precision of the geodetic receivers imply high costs, especially when many monitoring sites are required to cover the monitoring area and where there is a great risk of instrument damage or loss (Janssen and Rizos, 2003). This is often a severe constraint for the institutions and research communities with a limited budget and, in many cases, can discourage using the GNSS technique.

Recently, we have witnessed remarkable progress in the performance of low-cost GNSS chipsets and processing algorithms that manage the limitations of such hardware. The ubiquitous presence of low-cost GNSS receivers is a factor that can particularly stimulate innovations and thus open the door to new applications in different fields of engineering and science. Biagi et al. (2016) investigated the performance of single-frequency low-cost receivers in kinematic mode and detected horizontal displacement of 15 mm using a geodetic-class receiver as the base station. Cina and Piras (2015) examined the performance of low-cost single-frequency receivers and showed that they can be used for landslide monitoring under certain conditions. Caldera et al. (2016) presented that using a low-cost u-blox EVK-6T GPS receiver and a very short baseline of 70 m, a movement of a few millimetres can be detected when the daily solutions are processed. Paziewski (2022) demonstrated that low-cost receivers can offer code measurements with similar noise compared to high-grade receivers when the multipath effect is eliminated. He also confirmed that applying a survey-grade antenna instead of the patch one noticeably enhances the performance of low-cost receiver positioning.

This research continues the experimentation of low-cost receivers in geodetic deformation monitoring. We aim to assess the positioning accuracy of recent multi-frequency low-cost receivers. In particular, we investigate their applicability to deformation monitoring at a local scale and examine whether, when GNSS observations are processed in the state-of-the-art scientific software and with the optimal GNSS data processing strategy, they can achieve a level of accuracy close to that of high-grade receivers.

2. DATA AND METHODS

The study is based on the GNSS observations collected from different low-cost and high-grade receivers (Table 1). Five low-cost receivers, namely pairs of u-blox ZED-F9P, and Septentrio MOSAIC-X5 receivers, and a single SkyTraq receiver were used to collect the GNSS observations. First, the receivers were connected to the Trimble GNSS choke ring antenna TRM59800.00 NONE through an antenna splitter forming a zero-baseline set-up. They were installed as collocated stations and ran for three consecutive days. Then, the same receivers were connected in the same way to the patch u-blox ANN-MB antenna, and the measurements lasted two following days. In addition, in each campaign, a high-grade Trimble Alloy receiver was also installed and treated as a benchmark.

Table 1: Summary of the receiver and antenna sets used in the experiments.

Station name	Receiver type	Antenna type
SEP3	Septentrio MOSAIC-X5 S/N: 3607222	TRM59800.00
		u-blox ANN-MB
SEP6	Septentrio MOSAIC-X5 S/N: 3613856	TRM59800.00
		u-blox ANN-MB
SKY7	SkyTraq	TRM59800.00
		u-blox ANN-MB
UBL1	u-blox ZED-F9P S/N: #1	TRM59800.00
		u-blox ANN-MB
UBL9	u-blox ZED-F9P S/N: #2	TRM59800.00
		u-blox ANN-MB
TRI2	Trimble Alloy	TRM59800.00
		u-blox ANN-MB

The GNSS data were processed in a relative mode based on double-difference observations with fixed ambiguities in Bernese GNSS software v.5.2 (Dach et al., 2015). The reference station was one of the permanent stations of the Polish National Ground-Based Augmentation System (ASG-EUPOS) network, OPNT station, which was located about 13 km far from the measurement field. The OPNT station was equipped with a Trimble NETR9 receiver and TRM59800.00 SCIS choke ring antenna. GPS, GLONASS, and Galileo observations were processed in 24-h sessions with the 30 s sampling rate. To achieve the highest possible accuracy, first, it was necessary to develop an optimal processing strategy suitable for deformation monitoring with low-cost GNSS receivers. This was done by testing and selecting the most appropriate type of observations and their linear combinations, elevation cut-off angle, ambiguity resolution strategy, tropospheric delay modeling, and ionospheric delays handling. The optimal processing parameters chosen in this study are reported in Table 2. Three processing variants with the same settings and parameters were carried out for each set of receiver+antenna. The only difference was the satellite constellation used in the data processing, namely 1) GPS-only, depicted further in this manuscript as “G”; 2) GPS + GLONASS, “GR”; and 3) GPS + GLONASS + Galileo, “GRE”.

Table 2: Selected GNSS data processing parameters.

Constellations	GPS, GLONASS, Galileo
Observations	Double-differenced dual-frequency phase and code
Processing model	Relative, geometry-based
Elevation cut-off angle	3°
Orbits, clocks and Earth orientation parameters	CODE MGEX final products
Differential code biases for satellites and receivers	CODE monthly solution
Antenna phase center variations and offsets	Absolute IGS
Ocean tidal loading model	FES2004
Global ionosphere model	CODE final
Conventional models	IERS Conventions 2010
A priori tropospheric model	Global Pressure and Temperature (GPT) with Global Mapping Function (GMF)
ZTD parameter spacing	1 hour
Tropospheric gradient model	Chen&Herring
Gradient spacing	24 hours
A-Priori weights of tropospheric parameters	0.00001 m
Ambiguity resolution	SIGMA for L1/L2 observations

3. RESULTS OF DATA PROCESSING AND DISCUSSION

The experiment addresses a scientific question on the actual positioning performance of recent low-cost GNSS receivers. In particular, we focus on the impact of the employed antenna type and satellite constellation on the performance of the GNSS positioning for deformation purposes.

3.1. Statistics of the combined solution

An essential information about the positioning results gives a posteriori Root Mean Square (RMS) error. It is expected that a posteriori RMS error of relative GNSS positioning may reach about 1.0–1.5 mm when an elevation-dependent weighting scheme is used. A significantly higher RMS error indicates that the quality of GNSS data is poor, the data was collected under very bad conditions, or the preprocessing steps, such as cycle slip detection and correction, outlier detection, clock synchronization, etc., have not been successfully performed.

The top panels of Figure 1 depict a posteriori RMS errors calculated based on GNSS observations derived from different receivers connected to the TRM59800.00 chock ring antenna (in the left panel) and connected to the ANN-MB patch antenna (in the right panel). Two receivers plus a chock-ring antenna sets, namely UBL1 and SEP3 stations, achieved the a posteriori RMS slightly higher than 1.5 mm. It is clearly visible that the a posteriori RMS was much smaller for almost all stations when a chock ring antenna was employed. The improvement is from about 39% and 62% for SEP3, and UBL9 stations, respectively. For the

UBL1 station, the corresponding difference reaches about 3%. The only station with a slightly lower a posteriori RMS error when using a surveying-grade antenna is SEP6 (about 9%).

The bottom panels of Figure 1 show a chi-square statistics for the results obtained with the TRM59800.00 chock-ring and the ANN-MB patch antennas in the left and right panels, respectively. Similar to the a posteriori RMS error case, the lowest chi-squared values were obtained for receivers connected to the chock ring antenna. The chi-square indicator is below 1.5 for TRI2, SEP3, and UBL9 receivers, and the highest value of 3.2 is obtained for the UBL1 receiver. In the cases of the sets with the patch antenna, the chi-square values are almost always much higher. The only exception is the SEP6 station which achieves about 17% lower values of chi-square statistics. One can notice that there are no visible differences in a posteriori RMS error and a chi-square indicator between results derived from the same type of receivers (SEP3 vs. SEP5 and UBL1 vs. UBL9) when using the ANN-MB patch antenna. There are no significant differences between solutions using different satellite constellations in a chi-square statistic and a posteriori RMS error.

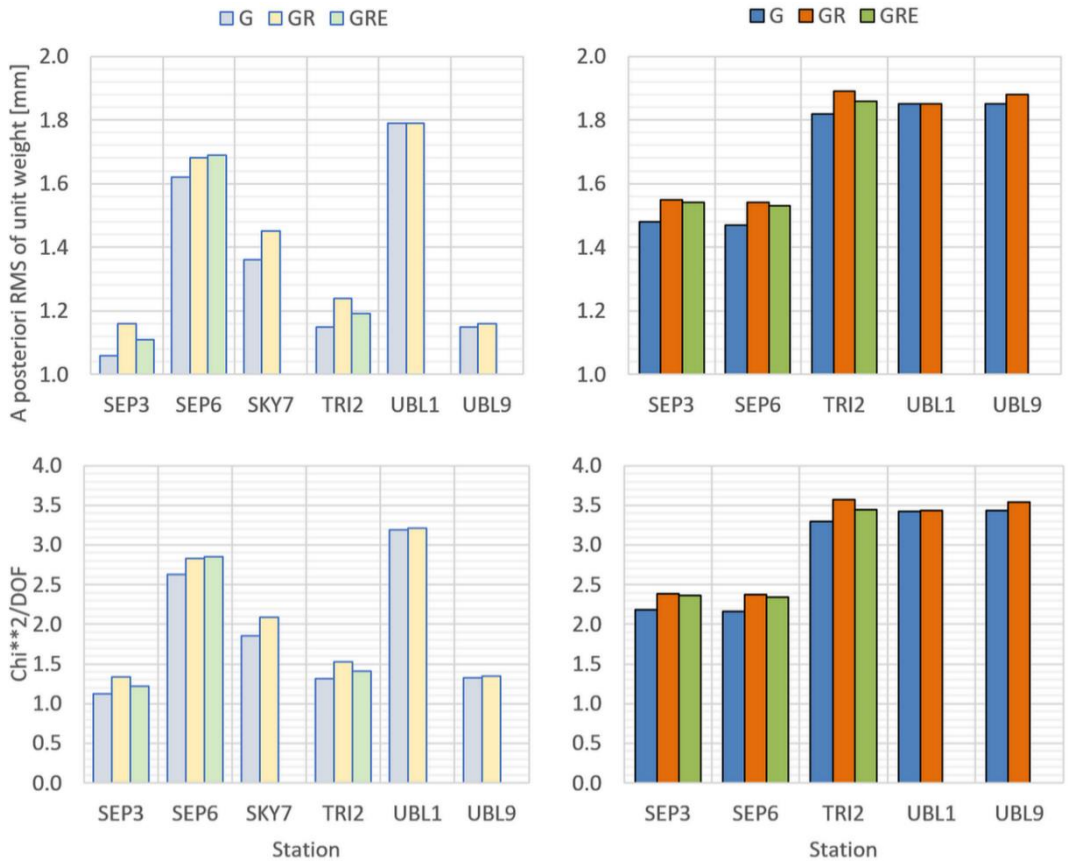

Fig. 1 A posteriori RMS error (top) and chi-square per degree-of-freedom (bottom), receiver + TRM59800.00 choke ring antenna sets (left), receiver + ANN-MB patch antenna sets (right).

3.2. Ambiguity resolution success rate

We processed the baselines separately one by one using the L1/L2 SIGMA strategy to resolve the ambiguities. Table 3 summarizes the ambiguity resolution success rates (ASR) obtained in analyzed processing variants. The highest ASRs were obtained for the OPNT-SKY7 baseline with the TRM59800.00 choke ring antennas at both ends, namely of 99.5% and 97.8% for GPS-only and GPS+GLLONASS solutions, respectively. In the cases of the baselines formed with the u-blox ZED-F9P receivers, the ASRs were at a similar level of about 90% for both processing variants, and the impact of antenna type does not appear to be strong. In the case of baselines formed to the stations equipped with the Septentrio MOSAIC-X5 receivers, we can observe that the ASRs level for GLONASS satellites is much lower than in the case of GPS and Galileo systems. Surprisingly, the ASR for GLONASS and Galileo observations is higher for the baseline to TRI2 station equipped with Trimble Alloy receiver than for the GPS system.

Table 3: L1/L2 ambiguity resolution success rate, mean over all daily sessions for each station [%].

Receiver + TRM59800.00 choke ring antenna sets								
Employed constellations:	**G**	**GR**			**GRE**			
Baseline/Constellation:	**G**	**G**	**R**	**GR**	**G**	**R**	**E**	**GRE**
OPNT-SEP3	93.4	94.4	74.0	86.4	94.2	73.7	100.0	89.6
OPNT-SEP6	92.5	94.0	68.4	83.1	95.1	68.7	95.5	86.8
OPNT-SKY7	99.5	99.1	96.8	97.8	-	-	-	-
OPNT-TRI2	87.9	89.6	97.4	92.5	89.8	96.7	98.7	93.8
OPNT-UBL1	90.1	90.1	81.2	88.7	-	-	-	-
OPNT-UBL9	85.5	86.3	94.9	87.4	-	-	-	-
Receiver + ANN-MB patch antenna sets								
Employed constellations:	**G**	**GR**			**GRE**			
Baseline/Constellation:	**G**	**G**	**R**	**GR**	**G**	**R**	**E**	**GRE**
OPNT-SEP3	95.1	95.1	73.9	85.9	94.8	73.0	98.3	88.8
OPNT-SEP6	95.1	95.5	73.5	85.9	94.8	73.0	98.3	88.6
OPNT-TRI2	95.9	96.5	96.5	96.5	96.2	95.1	93.0	94.9
OPNT-UBL1	90.7	91.0	98.6	92.2	-	-	-	-
OPNT-UBL9	91.7	90.2	80.5	88.8	-	-	-	-

3.3. Repeatability of estimated coordinates

The average repeatability of the estimated North, East, and Up coordinate components is given in Figure 2. The repeatability is calculated for each receiver+antenna set and each processing variant as the RMS error based on the final adjustment of the coordinates obtained for all processing sessions. As expected, the repeatability for horizontal coordinates is much higher than for the height component. There are no significant and evident differences in the

repeatability of coordinates between low-cost and Trimble receivers. In all cases, the coordinate RMS is below 1.5 mm, 0.5 mm, and 2.5 mm for North, East, and height components, respectively. There is also no clear impact of the antenna type on the coordinate repeatability. However, the impact of different systems used in the processing is apparent. In particular, the repeatability of coordinates is better when using multi-GNSS observations as compared to a single-system solution.

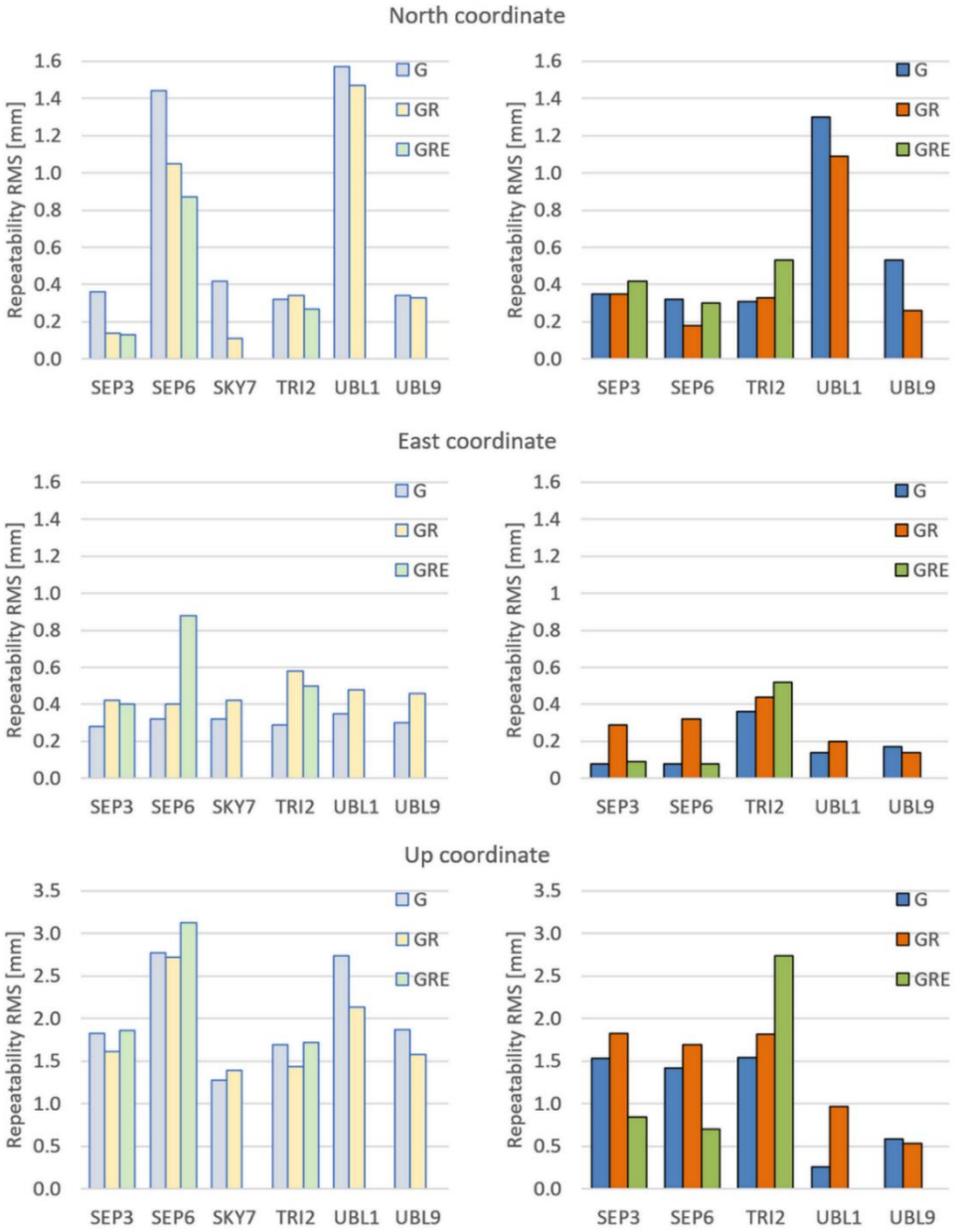

Fig. 2 RMS of coordinate repeatability in North, East, and height components for the baselines with TRM59800.00 choke ring antenna and ANN-MB patch antenna in the left and right panels, respectively.

Coordinate residuals of each solution (daily session) with respect to the combined solution computed for North, East, and Up components are reported in Table 4. The residuals allow identifying problems for individual stations or sessions. Table 4 shows that there are no cases when coordinate residuals reach an outstanding level for any processing variant. However, one can observe slight differences in computed residuals between processing variants. If we analyze the impact of the employed satellite observations, we can notice that the smallest residuals were usually obtained from the GPS+GLONASS processing variant.

Table 4: Residuals of coordinates for each daily session in milimetres.

Receiver + TRM59800.00 choke ring antenna sets										
	Station	**G**			**GR**			**GRE**		
		Ses. 1	**Ses. 2**	**Ses. 3**	**Ses. 1**	**Ses. 2**	**Ses. 3**	**Ses. 1**	**Ses. 2**	**Ses. 3**
N	**SEP3**	0.41	-0.17	-0.25	0.15	-0.08	-0.10	0.10	0.04	-0.14
	SEP6	-1.72	0.91	0.58	-1.21	0.74	0.44	-0.99	0.72	0.00
	SKY7	0.46	-0.35	-0.13	0.04	-0.10	0.13	-	-	-
	TRI2	0.33	-0.08	-0.30	0.39	-0.23	-0.17	0.30	-0.09	-0.21
	UBL1	-1.90	1.01	0.53	-1.70	1.18	0.26	-	-	-
	UBL9	0.37	-0.24	-0.21	0.36	-0.24	-0.19	-	-	-
E	**SEP3**	-0.36	0.12	0.10	-0.53	0.17	0.21	-0.51	0.19	0.17
	SEP6	-0.23	0.39	0.08	-0.40	0.18	0.37	-0.35	-0.61	1.02
	SKY7	-0.40	0.14	0.18	-0.52	0.18	0.23	-	-	-
	TRI2	-0.38	0.07	0.15	-0.70	0.13	0.40	-0.61	0.12	0.33
	UBL1	-0.33	0.31	0.19	-0.46	0.49	0.08	-	-	-
	UBL9	-0.38	0.06	0.19	-0.37	-0.24	0.49	-	-	-
U	**SEP3**	1.92	-1.72	-0.18	1.74	-1.45	-0.29	2.02	-1.61	-0.44
	SEP6	2.84	-2.69	-0.14	3.01	-2.21	-0.94	3.43	-2.69	-0.80
	SKY7	1.23	-1.32	0.10	1.58	-0.98	-0.61	-	-	-
	TRI2	1.78	-1.58	-0.17	1.55	-1.30	-0.23	1.83	-1.57	-0.29
	UBL1	2.72	-2.76	0.06	2.05	-2.22	0.18	-	-	-
	UBL9	1.91	-1.82	-0.06	1.79	-1.19	-0.60	-	-	-
Receiver + ANN-MB patch antenna sets										
	Station	**G**			**GR**			**GRE**		
		Ses. 1	**Ses. 2**		**Ses. 1**	**Ses. 2**		**Ses. 1**	**Ses. 2**	
N	**SEP3**	-0.32	0.15		-0.30	0.19		-0.38	0.17	
	SEP6	-0.29	0.13		-0.17	0.06		-0.29	0.08	
	TRI2	-0.30	-0.06		-0.09	-0.31		-0.50	0.16	
	UBL1	0.17	-1.29		0.10	-1.08		-	-	
	UBL9	-0.03	-0.53		-0.13	-0.23		-	-	
E	**SEP3**	0.05	0.06		-0.15	0.25		0.09	0.02	
	SEP6	0.04	0.07		-0.17	0.27		0.06	0.05	
	TRI2	-0.28	0.22		-0.36	0.25		-0.43	0.30	
	UBL1	-0.10	0.09		-0.12	0.16		-	-	
	UBL9	-0.09	0.14		0.00	-0.14		-	-	
U	**SEP3**	-1.07	1.09		-1.30	1.29		-0.54	0.64	
	SEP6	-0.99	1.01		-1.20	1.20		-0.45	0.53	

	TRI2	-1.05	1.13	-1.18	1.38	-1.82	2.05
	UBL1	0.12	-0.23	0.32	-0.92	-	-
	UBL9	0.24	-0.53	0.25	-0.47	-	-

3.4. Formal coordinate errors

Finally, the formal coordinate error estimates from each processing variant are computed and shown in Figure 3. Noticeable differences between receivers and processing variants are observed. It is seen that the application of multi-GNSS data processing reduces the formal error of each coordinate component regardless of the employed antenna type. When GLONASS and GPS observations are used, the formal error is reduced by an average of 22%, 14%, and 18% for the North, East, and Up components, respectively, for all receiver and antenna sets, except both u-blox receivers. The inclusion of Galileo observations resulted in an average accuracy improvement of 35%, 28%, and 32% for the North, East, and Up coordinates, respectively.

Considering the impact of the GNSS antenna, we can observe that using the ANN-MB patch antenna significantly increases the formal error of coordinates. This dependence is especially evident in the case of the UBL9 station equipped with the u-blox ZED-F9P #2 receiver. In this case, the formal error of coordinates is about 150% higher than when the patch antenna was employed compared to the solution with a geodetic antenna. The differences in the formal error using different antenna types for other stations are also significant. They reach up to 60% for the UBL1 station equipped with the u-blox ZED-F9P #1 receiver, and up to 80% for the SEPT3 station with the Septentrio MOSAIC-X5 one. The only station for which the impact of changing antenna type is much lower is the SEP6 station equipped with the Septentrio MOSAIC-X5 receiver. In this case, the increase of the formal error is only up to 15%.

We recall that formal coordinate accuracy estimates provided by the Bernese software are usually underestimated, mainly due to neglecting the physical correlations between observations or selected biases and errors in the physical models (Kashani et al., 2004).

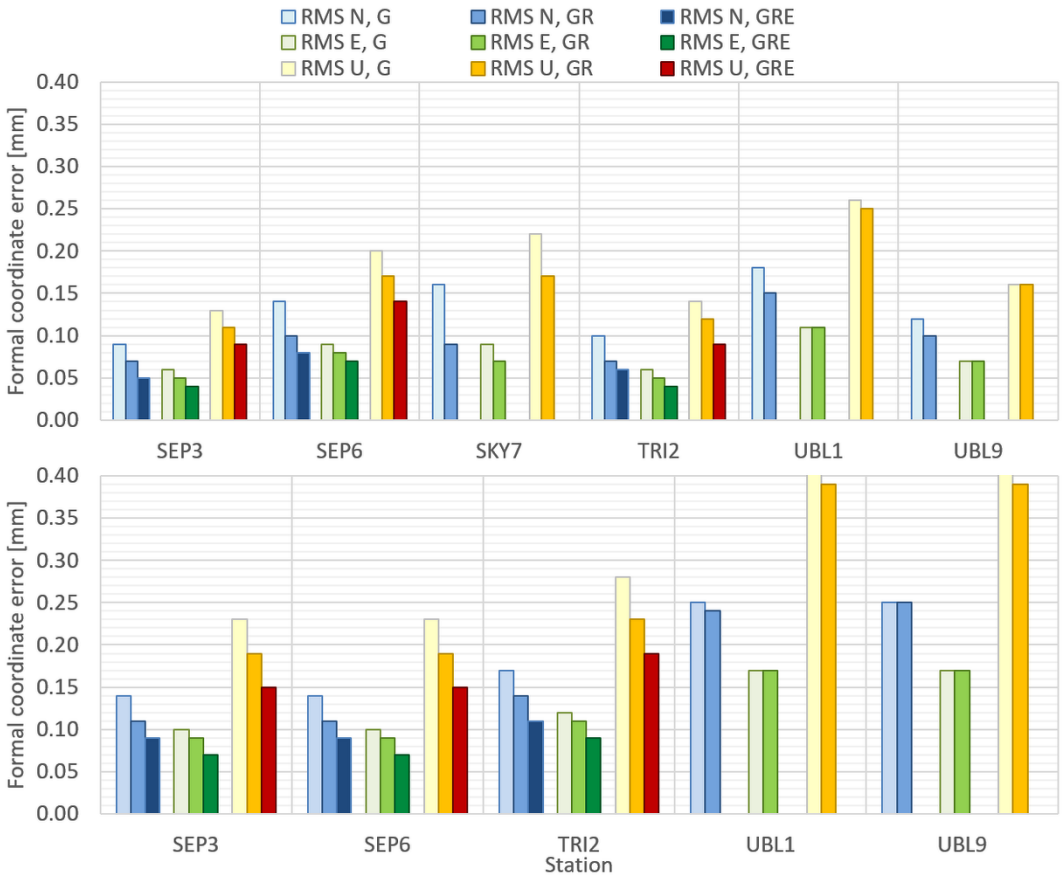

Fig. 3 Formal coordinate error for North, East, Up coordinate component. In the top panel are given the values for the baselines in which TRM59800.00 choke ring antenna was used, whereas in the bottom panel for the baselines which employed ANN-MB patch antenna .

4. CONCLUSIONS

This research assessed the positioning accuracy of recent multi-frequency low-cost receivers and their applicability to local-scale geodetic monitoring. We investigated whether GNSS observations collected from low-cost receivers can achieve a level of accuracy close to that of high-grade receivers.

We showed the significant impact of the GNSS antenna type on the precision of the coordinate estimates. We proved that applying a choke ring antenna instead of a patch one to a low-cost receiver can greatly increase the positioning accuracy.

The experiment also confirmed that the application of multi-GNSS data processing significantly reduces the error of estimated coordinates regardless of the employed antenna. The results of this study confirmed that with the optimal GNSS data processing strategy and the state-of-the-art scientific software, the latest low-cost receivers might be considered a mature complement to high-grade receivers in engineering applications, such as deformation monitoring.

REFERENCES

Baryla, R., Paziewski, J., Wielgosz, P., Stepniak, K., Krukowska, M., 2014. Accuracy Assessment of the Ground Deformation Monitoring with the Use of Gps Local Network: Open Pit Mine Kozmin Case Study. Acta Geodyn. Geomater. 11, 317–324.

Biagi, L., Grec, F.C., Negretti, M., 2016. Low-Cost GNSS Receivers for Local Monitoring: Experimental Simulation, and Analysis of Displacements. Sensors 16, 2140. https://doi.org/10.3390/s16122140

Caldera, S., Realini, E., Barzaghi, R., Reguzzoni, M., Sansò, F., 2016. Experimental Study on Low-Cost Satellite-Based Geodetic Monitoring over Short Baselines. Journal of Surveying Engineering 142, 04015016. https://doi.org/10.1061/(ASCE)SU.1943-5428.0000168

Cina, A., Piras, M., 2015. Performance of low-cost GNSS receiver for landslides monitoring: test and results. Geomatics, Natural Hazards and Risk 6, 497–514. https://doi.org/10.1080/19475705.2014.889046

Dach, R., Lutz, S., Walser, P., Fridez, P., 2015. Bernese GNSS Software Version 5.2. https://doi.org/10.7892/BORIS.72297

Janssen, V., Rizos, C., 2003. A mixed-mode GPS network processing approach for deformation monitoring applications. Survey Review 37, 2–19.

Kashani, I., Wielgosz, P., Grejner-Brzezinska, D.A., 2004. On the reliability of the VCV Matrix: A case study based on GAMIT and Bernese GPS Software. GPS Solutions 8, 193–199. https://doi.org/10.1007/s10291-004-0103-9

Larson, K.M., Poland, M., Miklius, A., 2010. Volcano monitoring using GPS: Developing data analysis strategies based on the June 2007 Kīlauea Volcano intrusion and eruption. J. Geophys. Res. 115, B07406. https://doi.org/10.1029/2009JB007022

Martín, A., Anquela, A.B., Dimas-Pagés, A., Cos-Gayón, F., 2015. Validation of performance of real-time kinematic PPP. A possible tool for deformation monitoring. Measurement 69, 95–108. https://doi.org/10.1016/j.measurement.2015.03.026

Paziewski, J., 2022. Multi-constellation single-frequency ionospheric-free precise point positioning with low-cost receivers. GPS Solut. 26, 23. https://doi.org/10.1007/s10291-021-01209-9

Wang, G., Kearns, T.J., Yu, J., Saenz, G., 2014. A stable reference frame for landslide monitoring using GPS in the Puerto Rico and Virgin Islands region. Landslides 11, 119–129. https://doi.org/10.1007/s10346-013-0428-y

ACKNOWLEDGMENTS

This study was supported by the project "Innovative precise monitoring system based on integration of low-cost GNSS and IMU MEMS sensors" POIR 01.01.01-00-0753/21, co-financed by the European Regional Development Fund within the Sub-measure 1.1.1 of the Smart Growth Operational Program 2014–2020.

BIOGRAPHICAL NOTES

Katarzyna Stępniak is an assistant professor of University of Warmia and Mazury in Olsztyn. Her main research areas focus on precise positioning, the application of GNSS to deformation monitoring, GNSS-based troposphere studies, and the use of GNSS observations in meteorology and climate applications.

Jacek Paziewski is an associate professor at the University of Warmia and Mazury in Olsztyn. His research interests include developing multi-GNSS positioning algorithms, modeling the ionospheric delays, smartphone and low-cost receiver positioning, and high-rate GNSS data processing.

Rafal Sieradzki is an associate professor at the University of Warmia and Mazury in Olsztyn. His research interest focuses on GNSS-based monitoring of ionospheric disturbances at high latitudes. He is also engaged in the development of algorithms to mitigate ionospheric delays in GNSS positioning.

Radoslaw Baryla is an assistant professor at the University of Warmia and Mazury in Olsztyn. His main research interests include the application of GNSS to surveying engineering, precise leveling, and deformation monitoring.

CONTACTS

Katarzyna Stępniak
University of Warmia and Mazury in Olsztyn
Oczapowskiego 1
10-719 Olsztyn
POLAND
katarzyna.stepniak@uwm.edu.pl

Jacek Paziewski
University of Warmia and Mazury in Olsztyn
Oczapowskiego 1
10-719 Olsztyn
POLAND
jacek.paziewski@uwm.edu.pl

Rafał Sieradzki
University of Warmia and Mazury in Olsztyn
Oczapowskiego 1
10-719 Olsztyn
POLAND
rafal.sieradzki@uwm.edu.pl

Radosław Baryła
University of Warmia and Mazury in Olsztyn
Oczapowskiego 1
10-719 Olsztyn
POLAND
baryla@uwm.edu.pl